# Penetration of turbulence into a gravel bed: informing models of hyporheic exchange

**Danial Iskandar Nordinson**
University of Melbourne, Melbourne, Australia
daniala@student.unimelb.edu.au

**Matthew Timothy Oka**
University of Melbourne, Melbourne, Australia
moka@student.unimelb.edu.au

***Abstract***: *The hyporheic zone is the porous region beneath and adjacent to streams, in which ground and surface water interact. A multitude of organisms rely on the hydrological interaction occurring in this region, as it purifies stream-water, cycles nutrients and influences the spread of contaminants. Two dominant hyporheic exchange mechanisms have been identified in stationary beds: advective pumping and turbulent dispersion, which are driven by either hydrostatic or dynamic pressure variation at the sediment-water interface respectively. Through flume experiments, we characterise the turbulent component of hyporheic exchange. By analysing the frequency spectrum measured throughout the sediment bed, we identify dominant frequencies (each representing turbulent dispersion) and examine the decay of such turbulence as it penetrates into the sediment. Many current models of hyporheic exchange are founded on the assumption of limited turbulence within the stream bed. We show that gravel beds act as low pass filters—with low frequency components of turbulence penetrating deeper into the stream bed than higher frequency components. Consequently, assumptions of limited turbulent penetration used in many current hyporheic exchange models may not be valid, particularly in flow regimes with strong low frequency components. Findings from our experiment will therefore inform and improve the application of hyporheic exchange models.*

## Introduction

The hyporheic zone forms the porous region immediately below and adjacent to streams. Hyporheic exchange includes the advection of fluid and the transfer of chemicals (such as nitrogen (Triska, Duff & Avanzino, 1993), dissolved oxygen (O'Connor & Hondzo, 2008), nutrients (Bardini, Boano, Cardenas, Revelli & Ridolfi 2012)), and heat (Cardenas & Wilson, 2007) across the sediment-water interface (SWI). Consequently, these transfer mechanisms are ecologically important; with a range of biota relying on this exchange, including spawning fish (Baxter & Hauer, 2000), shrimp (Richardson & Humphries, 2010), macroinvertabrates (Boulton, Datry, Kasahara, Mutz, & Stanford, 2010) and general microbial ecology (Hendricks, 1993). Furthermore, depending on the bed composition, these processes can facilitate the immobilisation of contaminants through mechanisms such as colloidal deposition (Ren & Packman, 2004); thus influencing water quality and stream health (Bencala, 2006). Identified as an ecotone between surface water and sub-surface biomes (Brunke & Gosner, 1997), the hyporheic zone is also an interstitial habitat for a wide range of organisms that migrate temporarily into this region during adverse conditions (Brunke & Gosner, 1997). The exchange processes are fundamental to river ecology (Stanford & Ward, 1988); not only along its banks (Lambs, 2004), but also across floodplains and between meanders (Wondsell & Swanson, 1999). As such, hyporheic exchange is recognised as a significant function in overall stream health (Boulton, Findlay, Marmonier, Stanley, & Valett, 1998).

As individual hydrological features, the importance of both streams and groundwater are well-recognised, and the processes occurring in either feature have been documented comprehensively (Buss et al., 2009). However, despite fluid interchange across the SWI being studied since at least the late 1940s (Vaux, 1962), there remains significant knowledge gaps in this field (Buss et al. 2009). Boulton et al. (1998) suggest that the distinct perspectives of ecologists and hydrologists on streams and groundwater (respectively) is partly to blame for such research barriers. And while the motivation of study in the hyporheic zones is due to the biological, chemical and mass transport processes occurring here, it is widely agreed that overcoming the existing knowledge gaps cannot be achieved by a single discipline alone; but through a holistic, interdisciplinary approach (Poole, Stanford, Running & Frisell 2006; Gerbersdorf, Hollert, Brinkmann, Wieprecht, 2011; Krause et al, 2011). Furthermore, advancement in understanding hyporheic zone processes requires novel approaches based on both "intensive micro-scale and long-term baseline empirical studies, and modelling approaches" (Krause et al., 2011, p. 495).

Although there is a necessity to pursue a comprehensive interdisciplinary approach, it is fundamental to understand the most basic dynamic processes occurring in these systems. Advection, turnover and turbulent dispersion (Packman & Bencala, 2000) have been identified as the main processes by which hyporheic exchange occurs—with the most widely used exchange models (Elliott & Brooks, 1997a; Boano et al., 2011; Zhou & Mendoza, 1993) derived from these principles. While these processes have been extensively researched, the relative contribution of each mechanism is still poorly understood (Packman et al., 2004). In particular, the effect of stream turbulence penetrating into the sediment bed has been largely ignored by many popular pumping models (see Elliott & Brooks' (1997a) advective pumping model). Even models developed explicitly for turbulent hyporheic exchange (see Boano et al., 2011) assume that turbulent penetration is confined to relatively shallow sections of the bed.

The purpose of this paper is to identify dominant frequencies attributed to turbulence penetration and characterise the rate of decay of the amplitudes of these signals as they travel deeper into the sediment column. We hypothesise that turbulent penetration is not necessarily limited to shallow regions of stream beds, especially in flows with low frequency components. Through experiment we show that coarse sediment acts as a low pass filter, meaning low frequency turbulence decays the least as it moves through the sediment matrix. This implies that fundamental assumptions for many hyporheic exchange models, particularly the assumption of Darcian flow directly beneath the SWI, are not entirely accurate.

To investigate this, we employed a gravel bed flume experiment with pressure transducers of varying height to track turbulence decay within the sediment bed. In this paper, we first provide a review of existing literature into existing hyporheic exchange models, followed by our experimental research method and accompanying analysis, and finally a discussion of our findings in the context of existing bodies of work. In our research we characterise this turbulence—as a single component of hyporheic flow—penetrating into the sediment bed. Findings from our research will support ongoing research in this field, with broader implications in river management (Buss et al., 2009) and restoration design due to increased urbanisation (Finkenbine, Atwater, & Mavinic, 2000; Hancock, 2002; Crispell & Endreny, 2009).

# Literature Review

## Physical processes of hyporheic exchange

It is widely recognised that hyporheic exchange results primarily from advection, turnover and turbulent dispersion. Hyporheic processes often occur simultaneously, with their relative significance in overall exchange dependent on flow regime and stream conditions. While the focus of this paper is primarily on the turbulent component of hyporheic exchange, the high interdependence of processes indicates they must all be considered.

Advection processes result from pressure differentials along the SWI, often caused by stream bedforms. Under such conditions, flow is driven into the sediment at regions of higher pressure and drawn out at regions of lower pressure. Wörman, Packman, Johansson & Jonsson (2002) have shown that advection processes are often a result of bedforms, with topography inducing local pressure differentials that in turn drive flow through the sediment. Thibodeaux and Boyle (1987) have used tracers to demonstrate this process in gravel-bed experiments. Similarly, Packman et al. (2004) found that hyporheic exchange in a fixed bedformed flume was well represented by advective pumping models.

Elliott and Brooks (1997b) also identified turnover as another important mechanism for hyporheic exchange in mobile bedforms. This occurs when the movement of bedforms releases trapped pore water; contributing to hyporheic flows. Most commonly, subcritical flow in streams causes scour and deposition on the upstream and downstream sides of bedforms respectively. This alternating process of scour and deposition causes mixing of interstitial fluids and stream water (Packman & Brooks, 2001). In streams with fast moving beds, turnover effects have often been found to dominate hyporheic exchange (Packman & Brooks, 2001). However, with slow moving beds the reverse is true and turnover-induced exchange becomes insignificant (Elliott & Brooks, 1997b; Packman & Brooks, 2001). In this experiment we propose a stationary bed, thereby eliminating effects resulting from turnover.

The final mechanism, turbulent dispersion, occurs when there is a momentum transfer across the SWI; inducing a non-zero slip velocity at the interface. Zhou and Mendoza (1993) suggest that this is the result of turbulent coupling of surface and pore water flows. This mechanism was observed by Nagaoka and Ohgaki (1990) when conducting flat-bed flume experiments in the absence of advective pumping pressures. It has since been identified as an important driver of hyporheic exchange; becoming increasingly important as bed porosity and sediment size increase. In flume experiments with coarse sediment, Shimizu, Tsujimoto & Nakagawa (1990) found that large slip velocities would be generated at the SWI. Packman et al. (2004) infer that in such conditions, turbulent dispersion is likely to be the dominant mechanism of hyporheic exchange.

## Importance of turbulence

Turbulent flow is defined as one which is disordered in time and space, with a wide range of spatial wavelengths (Nikora, 2010). Under turbulent conditions, mixing of substances and transported quantities occurs much faster than molecular diffusion processes alone (Lesieur, 2008; Pope, 2000). Turbulence, in some form, is present in every natural stream environment (Davidson, 2004), and hence forms an influential part of hyporheic exchange. As current research has found turbulent coupling to be increasingly important in coarse sediment beds, there is a large range of physical applications, particularly in river environments, where this mechanism is likely to dominate. Indeed, in transitional and rough beds—as are commonly found in natural streams—Reidenbach, Limm, Hondzo and Stacey (2010) have found turbulent dispersion to be the primary mechanism for mass exchange. Although it is often difficult to differentiate between the above physical processes when analysing experimental data, turbulent dispersion mechanisms are expected to decay with depth (Packman et al., 2004). Similarly, current research by McCluskey et al. (in prep.) suggest that turbulent dispersion mechanisms dominate in the upper sediment layers—although both advective and turbulent processes are required for bedform-induced hyporheic exchange to occur. Therefore, turbulence can be recognised as a highly important aspect of hyporheic exchange.

## Turbulence in sediment beds

Turbulence found beneath the SWI can be generated in two ways: locally within the sediment pores, or externally in the free stream. Detert, Nikora and Jirka (2010) have shown that locally-generated pore turbulence is predominantly characterised by high frequencies (in the range of 50-60Hz), especially when compared to the 2-4 Hz dominant free stream turbulence frequencies measured by Venditti and Bennett (2000). In the context of the hyporheic zone, we contend that low frequency turbulence is able to best penetrate the sediment matrix. If a non-instantaneous transmission of pressure within the sediment bed is assumed, then slow, low frequency components of turbulence can be expected to penetrate further due to their prolonged application. We therefore maintain that the lower frequency turbulence generated in the free stream is the primary driver of turbulent hyporheic exchange.

## Hyporheic exchange models

There have been a number of models developed for hyporheic exchange; each derived from knowledge of the various physical processes described above. However, many of these models overlook or make gross assumptions regarding the role of turbulent mechanisms. This section examines key exchange models; identifying areas where each may be informed by an improved understanding of turbulence.

### Advective pumping models

Elliott and Brooks (1997b) propose a two-dimensional pumping model for purely advective hyporheic exchange. This model is founded entirely on advective processes, although the same paper also proposes a complementary model for turnover effects. In the advective model the pressure distribution for triangular bedforms is thought to be represented by a sinusoidal boundary condition, given by:

$$h = h_m sin(kx) \quad (1)$$

Where $h$, the dynamic head, is a function of $h_m$, the amplitude of the dynamic head fluctuations at the bed surface (defined by Fehlman (1985) for triangular bedforms), $k$ is the wave number related to bedform wavelength, and $x$ is the horizontal coordinate.

Coupling this pressure distribution with Darcy's Law across a porous medium and assuming a homogeneous, isotropic bed means dynamic head and pore water velocity can be solved using the Laplace equation. The resulting velocity field is as follows:

$$u = -u_m \cos kxe^{ky} \quad (2)$$

$$v = -u_m \sin kxe^{ky} \quad (3)$$

Where $u$ is the longitudinal pore water Darcy velocity, $u_m$ is the pore water Darcy velocity scale (a function of the hydraulic conductivity of the bed, wave number and $h_m$), $y$ is the vertical coordinate and $v$ is the vertical Darcy velocity.

Under this model, pressure differentials along the SWI drive water into and out of the sediment causing hyporheic exchange. This model is based on an infinite bed, however Packman, Brooks and Morgan (2000) refined this model for application to finite beds. This model was further refined by Tonina and Buffington (2007) for three-dimensional applications in less sinusoidal bedforms. The assumption of a planar bed and sinusoidal pressure variation was removed, in favour of direct measurement of the SWI pressure distribution.

Variations of this model have often been employed: Cardenas and Wilson (2007) and Bardini et al. (2012), for example, numerically solve Navier-Stokes equations to determine the appropriate boundary conditions before employing similar subsurface analysis. Such variations may be considered more representative of near-bed turbulent conditions within the water column as they do not rely on assumptions of sinusoidal pressure distributions.

A key assumption of these models is that Darcian flow can be assumed below the SWI. However, in regions where turbulence is considerable, non-linear dynamics will take place making this approach invalid. Thus, where significant turbulent penetration is evident across large regions, the application of advective pumping models is inappropriate.

### Turbulent pumping models

A turbulent model proposed by Boano, Revelli and Ridolfi (2011) modifies and develops Elliott and Brooks' (1997a, b) pumping model for application in turbulent conditions. This assumes a dynamic head distribution at the SWI can be characterised by a single sinusoidal wave. That is, although head distribution is most accurately described as an infinite sum of sinusoidal waveforms, Boano et al. (2011) contend that as the largest wavelength harmonics penetrate the deepest, these govern exchange. By using such a waveform to impose pressure boundary conditions, Darcian flow can then be assumed in the bed—yielding the velocity field equations (2) & (3) shown above.

The use of Darcian flow in this model is predicated on the assumption that non-linear turbulent effects are limited to a relatively shallow portion of the sediment bed and are hence negligible when considering a deep sediment column. As with the pumping model, this assumption may be invalid if turbulence is found to penetrate deep into the sediment bed. Furthermore, while the assumption that larger wavelengths penetrate deepest are supported by numerical modelling (see Higashino & Stefan, 2008), there is little experimental research in this area to date. A greater understanding of the characteristics of turbulent waveforms travelling into the sediment bed will further inform such models and justify the assumptions made regarding the extent of its contribution to hyporheic exchange.

### Coupled free stream/sediment flow

Zhou and Mendoza (1993) developed a coupling model for gravel bed streams derived from models of flow over impervious beds. The porosity of the bed materials leads to a slip-velocity at the SWI, which penetrates into the stream bed. Similarly, momentum exchange also occurs between the pore water and penetrating stream water. In this model, near-bed flow velocity is measured and assumed to decay exponentially with depth—with results feeding into continuity and Navier-Stokes equations. The solving of these equations gives the subsurface flow velocities. Such models are yet to be comprehensively validated against experimental data, and hence could benefit from our experimental findings.

### Velocity pulse models

Higashino and Stefan (2008) developed a velocity pulse model to estimate turbulent penetration in the vertical direction. In this model, turbulence in the free stream is broken down into a set of sinusoidal waveforms that can be analysed individually. As with Boano et al. (2011), the dominant waveforms can be identified and used for analysis. These are represented as a velocity pulse at the SWI—which is thought to have non-zero vertical velocity components. By making use of fluid continuity and incompressible flow assumptions, Higashino and Stefan (2008) are able to simulate the penetration behaviour of in-stream turbulence in terms of vertical fluid velocity. Computer simulations of these models suggest that sediment acts as a low pass filter; that is, low frequency waveforms penetrate deeper into the sediment, and the damping of vertical velocity components increase with frequency. While this model does not directly result in a velocity field or mass transfer characteristics, it yields important insights into the way turbulence penetrates into a sediment bed. In their numerical velocity pulse simulations, Higashino and Stefan (2008) found that a high frequency pulse of 1000Hz was found to decay to less than 20% of the initial velocity amplitude after traveling only 0.001cm into the sediment. These findings support our hypothesis regarding turbulent behaviour, however as they have only been numerically simulated, there are research opportunities to evaluate these mechanisms experimentally.

### Effective diffusion models

Packman et al. (2004) propose that the combined effects of turbulence and advection in hyporheic exchange can be modelled using an effective diffusion coefficient (D), which is dependent on stream depth ($d$), characteristic sediment diameter ($d_g$), Reynolds number ($R$), bed depth ($d_b$), kinematic viscosity ($v$) and stream velocity, as seen in Equation 4.

$$D/_v = f\left(R.{}^{d}/_{d_b}.{}^{d_g}/_{d_b}\right) \tag{4}$$

O’Connor and Harvey (2008) developed an empirical relationship for the effective diffusion coefficient based on meta-analysis of past experiments. This relationship was further refined by Grant, Stewardson and Marusic (2012). In addition, two new empirical relationships for effective diffusion coefficients through multi-linear regression were developed (Grant et al., 2012). Rather than solve for a flow-field below the SWI, effective diffusion models account for the change in concentration in the sediment over time. However, a criticism of such models is that they lump many mechanisms and properties together as a single process. A better understanding of the contribution of turbulence will alleviate some uncertainty in this area.

### Synthesis

Current modelling techniques can benefit significantly from an improved understanding of turbulent penetration. In particular, due to the often used advective and turbulent pumping models having similar origins, both are underpinned by assumptions of limited turbulence penetration into the stream bed. Our research aims to inform the application of these models. The benefit of these models is that they can be accurately applied once the turbulence contribution has become sufficiently weak. Our experiment determines the spatial scale at which turbulence is filtered, allowing for the improved application of these models by redefining the bounds in which they are relevant.

Both the coupled free stream/sediment flow and velocity pulse models characterise turbulent decay, and would benefit from an improved understanding of this process. Although the coupled free stream/sediment flow model has been fitted against some experimental data (Zhou & Mendoza, 1993), none of the experiments used were explicitly focused on measuring the decay of turbulence. This may also be due to the primary focus of this model being the macroscale flow through the bed. Our research therefore explores the usefulness of these models by understanding turbulence penetration in a section of the sediment column and relates our findings to the entire sediment bed.

In contrast to the above models, effective diffusion models incorporate all hyporheic processes into the calculations. However, in doing so, the relative importance of each process is difficult to ascertain. Our experiment helps to elucidate the importance of turbulence which is often obscured in many of these models.

## Methodology

As discussed previously, the study of the hyporheic zone requires an interdisciplinary approach, and while our research focuses on characterising turbulent penetration into the sediment bed, it is reasonable to suggest that potential hydrological, ecological and chemical inferences may arise from such studies. Work by Packman et al. (2004) has shown that the turbulent contribution to bulk pore water velocity decays exponentially with depth of the bed, however our research further elaborates the characteristics of such penetration at a local scale. By comparing dominant frequencies (attributed to turbulence) present at the SWI with measurements deeper in the bed, we identify dominant signal frequencies, their decay rate into the bed, and therefore the effectiveness of the sediment bed as a low pass filter. As both triangular and sinusoidal bedforms further induce hyporheic flows on the lee side of the dunes (Boano, Revelli & Ridolfi, 2007), our research considered a simple flatbed scenario as well as a sinusoidal bedform. Research in this area will better inform the usefulness of existing hyporheic exchange models across varying bed types.

This research has been conducted from a critical perspective; drawing on works that examine turbulent penetration into gravel beds, but in the context of its application to hyporheic models that combine advective pumping and coherent turbulent advection. An examination of existing literature on hyporheic exchange has shown that significant gaps remain in how these mass transfer processes interact (McCluskey, Stewardson & Grant, in prep.) and the extent of turbulent contribution. While the intent of this research is not to attempt to resolve this directly, analysis of penetrating turbulence signals will further develop current understanding of the ability of porous, subsurface flow to respond to pressure fluctuations occurring at and above the SWI (Cardenas & Jiang, 2011).

## Methods

### Experimental Set-up

The following experiment forms part of broader research conducted by McCluskey et al. (in prep.) to investigate hyporheic exchange mechanisms. The experiment was therefore largely designed by those authors, although adjustments were made to suit the research objectives of this paper.

#### Flume configuration

Our experiment was performed using a rectangular, recirculating flume. Recirculating flumes have been shown to be useful in hyporheic research, as they allow excellent control of water flow, bedform and channel gradient, while also having the advantage of minimising water wastage. The recirculating flume was chosen in preference to in-situ testing as it was deemed more appropriate for identifying and controlling particular processes. The flume set-up is shown in Figure 1. The sediment length within the flume was 4.8m (measured between the upstream tank and downstream lip), with average sediment cross-section dimensions of 0.29m by 0.3m. At the end of the flume and at the return pipe, sediment filters were fitted to collect mobile sediment particles and to protect the pump from excessive damage. To replicate ideal conditions for turbulent penetration a coarse homogenous gravel was used. The gravel used across all experiments were measured to have a median particle size ($d_{50}$) of 5.9mm and porosity of 43.8%.

## Sensor configuration

To minimise signal reflection from both upstream and downstream sources, and to allow the water to settle into the desired uniform flow regime, an array of 16 digital pressure transducers were positioned midway down the flume. The spacing between sensor midpoints was 1.5cm (as limited by the width of the transducers) and were positioned at nominal depths for each run; thereby capturing pressure signals at various heights from the SWI to the flume bed.

For each experiment the following could be varied: bedform, slope, flowrate and sensor depth. The bed was either flattened parallel to the flume base or moulded into a sinusoidal form with a 280mm wavelength and 20mm amplitude; thus altering the flow profile within the stream. Bed slope was varied between 0 and 1% with corresponding flowrates of 4.5 and 8.3L/s. For each experiment, all sensors were set to a uniform depth beneath the SWI; deepening the sensors by approximately 100mm between experiments. Table 1 summarises how the flume was set up for each experiment. Varying the bed configuration and flow profiles allowed for investigation of different stream flow and imposed turbulent boundary conditions.

It is worth noting that herein, the term *configuration* will be used to refer to the set of experiments undertaken for a given bed-type and slope. Each configuration consists of four individual experiments, or runs. For example, Configuration 1a refers to all experiments conducted on a sinusoidal bed at 0% slope. Each configuration includes four individual experiments with the sensor depth below the SWI changed between each.

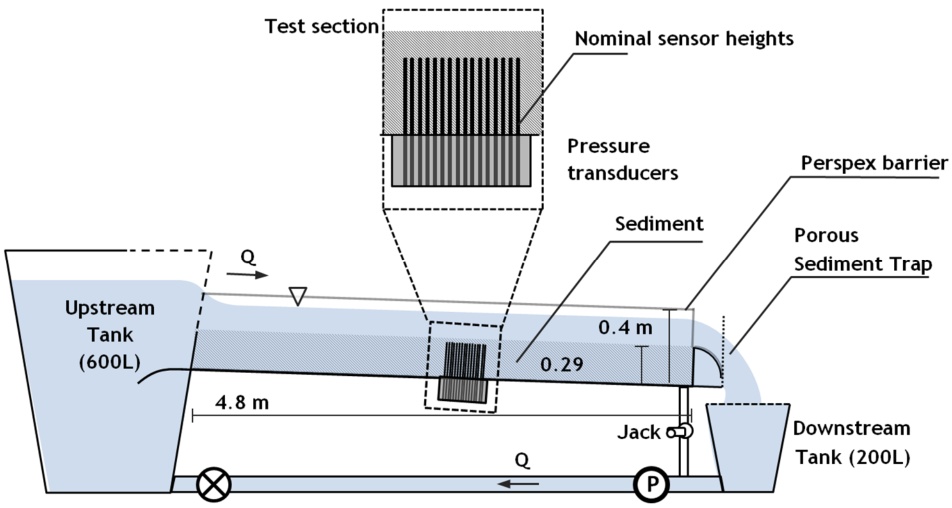


**Figure 1: Flume experiment set-up (image adapted from McCluskey, et al., in prep)**

## Sampling rate and frequency

In reference to the above literature review, pressure signals of most interest to us were determined to be less than 40Hz (Detert, Nikora, & Jirka, 2010). Therefore, to ensure this range was captured while leaving scope for investigation at higher frequencies, each experiment was run for 5 minutes at a sampling rate of 250Hz. As will be discussed subsequently, this means a frequency range of up to 125Hz may be analysed. If the recorded spectrum appeared to contain dominant frequencies up to

125Hz, increasing the sample rate was also possible. Signals recorded by the digital sensors were recorded directly to a desktop computer.

**Table 1: Summary of experimental runs, showing bed type, slope and sensor depth**

| Run # | Configuration # | Bed type | Slope | Flowrate | Sensor depth (from SWI) |
|---|---|---|---|---|---|
| 1 | 1a | Sinusoidal λ=280mm, a=20mm | 0% | 4.5L/s | 0mm |
| 2 | | | | | 100mm |
| 3 | | | | | 200mm |
| 4 | | | | | 280mm* |
| 5 | 1b | | 1% | 8.3L/s | 0mm |
| 6 | | | | | 100mm |
| 7 | | | | | 200mm |
| 8 | | | | | 280mm* |
| 9 | 2a | Plane | 0% | 4.5L/s | 0mm |
| 10 | | | | | 100mm |
| 11 | | | | | 195mm |
| 12 | | | | | 280mm |
| 13 | 2b | | 1% | 8.3L/s | 0mm |
| 14 | | | | | 100mm |
| 15 | | | | | 195mm |
| 16 | | | | | 280mm |

*Denotes mean sensor depth.

## Analysis

### Data collection and filtering

For each sampling period corresponding to the runs identified above, gauge pressure time series from each transducer (measured in voltage) were outputted directly to MatLab. From this data, the base-line sample (taken prior to the experiment) was subtracted to remove pressure differences between the sensors. The resulting recordings were then converted from voltage to pressure by using calibration charts provided by the sensor manufacturer.

From lab notes taken at the time of each experiment, the runs that were likely to have the highest quality measurements were selected for analysis. For each sensor, these were further broken down via a Reynolds' decomposition to determine the pressure fluctuations attributable to turbulence (Equation 5).

$$p'(t) = p(t) - \bar{p} \tag{5}$$

Where $p(t)$ is the pressure, $\bar{p}$, the mean pressure and $p'(t)$, the turbulent pressure fluctuations about the mean at each sensor.

The resulting unfiltered turbulent pressure fluctuations at each sensor were then plotted against time, and the plots inspected for signs of clearly recognizable systematic errors—such as leaks (indicated by sudden periodic dips in pressure), or outputs well outside the range of neighbouring sensors. Such sensors were noted and excluded from subsequent analysis.

Pressure fluctuations at each sensor were further analysed for each experiment by way of a Fourier transform. By definition, the resolution of the data following such an analysis is reduced to half the sampling rate—meaning the decomposed function yielded amplitudes for the frequency range of 0 to 125 Hz.

A Fourier amplitude spectrum was constructed for each sensor, and each compared between runs and configurations. From this, the frequencies of interest were further refined. As discussed previously, it was identified by Detert et al. (2010) that turbulence was likely characterised by frequencies between 0 and 40Hz, however following visual inspection little activity was found to occur beyond 30Hz. As such, the range of interest was narrowed between 0 and 30Hz. As proven effective by Detert et al. (2010), smoothing using a sixth-order Butterworth filter was applied, in this case, to the signal data between the ranges of 0.05 and 30Hz—thereby excluding frequencies outside our desired range. Furthermore, to represent the relative increases in frequencies in a more uniform manner, a log scale was used along the frequency axis.

### Principal component analysis

Utilising filtered data, each run was analysed using empirical orthogonal functions (EOF), also known as the process of principal component analysis (PCA). The purpose of this is to spatiotemporally correlate the turbulence readings at each sensor location, for each run, so the underlying signals can be analysed. EOF analyses have previously been successfully utilised in hyporheic exchange modelling (for example, see Cardenas & Jiang, 2011). The result is four EOF outputs per configuration.

The EOF determines a number of linearly independent modes of variance that are present at all sensors. The maximum number of modes of variance is limited by the number of sources of variance, or in this case, input sensors. Hence for each run, the maximum amount of modes of variance is 16, less the number of excluded sensors.

Using this function, the sensor data for each run was decomposed into sets of linearly independent EOF modes; each representing some percentage of the variance over the entire run. Equation 6 below, shows how the sensor data is decomposed into EOF modes.

$$p''_{run}(t, x_N, y_n) = \sum_{i=1}^{k} PC_{N,i} \cdot E_i(t) \tag{6}$$

Where $p''_{run}$ represents the turbulent pressure data for each run, varying with time, $t$, sensor position in the x-plane ($x_N$) and in the y-plane ($y_N$). $k$ is the number of non-excluded sensors, $PC_N$ is the principal component and $E_i(t)$ is the time series corresponding to each mode of variance.

The principal component output is a single scalar unit for each sensor location and mode—it represents the magnitude of a particular time series at each point. The time series output is a time varying coefficient representing each mode of variance. The time series is maintained between sensor locations, and hence each mode represents a statistically independent signal being observed at all points. Another output accompanying each mode is the variance explained (also known as expected variance). This shows how much of the observed variance can be explained by a particular mode. By definition, Mode 1 represents the mode in which the greatest amount of variance can be explained, with the explained variance decreasing with mode number.

For this analysis, only Modes 1 to 4 for each experimental run were considered. As will be discussed later, these four modes were found to explain a great portion of the variance in the data. Analysis was conducted using scripts adapted from McCluskey et al. (in prep.)—with the resulting time series and principal component data feeding into subsequent analysis. A weakness of the PCA is that it does not necessarily link directly to a physical observations. However, coupled with an understanding of the expected processes, it yields valuable statistical insights into underlying processes across a spatial domain.

### Surface plots

For each configuration, the time series EOF outputs for the four individual runs were utilised. Via a Fourier transform, these time series values were broken down into corresponding amplitude and frequency components. Again these were in the range of 0 to 125Hz, although due to the previously applied filter, only the range of 0.05 to 30Hz contained data for our research.

The underlying assumptions of the surface plot analysis is that the calculated modes are comparable between runs. This can be considered valid if the proportion of variance explained by a particular mode is similar between runs. Hence, prior to the surface plotting, the cumulative expected variance for each run within a configuration was plotted against mode to allow for comparison.

Following this, MatLab was used to construct an interpolated surface plot linking the four Fourier outputs against depth. In these graphs, the x and y axes show frequency and depth below the SWI respectively, while the amplitude of the signal is represented in colour. It should be noted that as this amplitude results from a decomposition of the EOF time series, the colour scale is dimensionless, despite being indicative of turbulence strength at a particular frequency. From these, the changes in signal strength can be visualised against both depth and frequency. Hence, the general behaviour of the various turbulence components can be observed against depth.

## Results

Figure 2 shows the resulting cumulative variance explained for each mode and configuration, while Figure 3 shows the resulting surface plots for the primary mode of variance. Surface plots for additional Modes 1 to 4 for each configuration are not shown, however the same pattern can be observed in each.

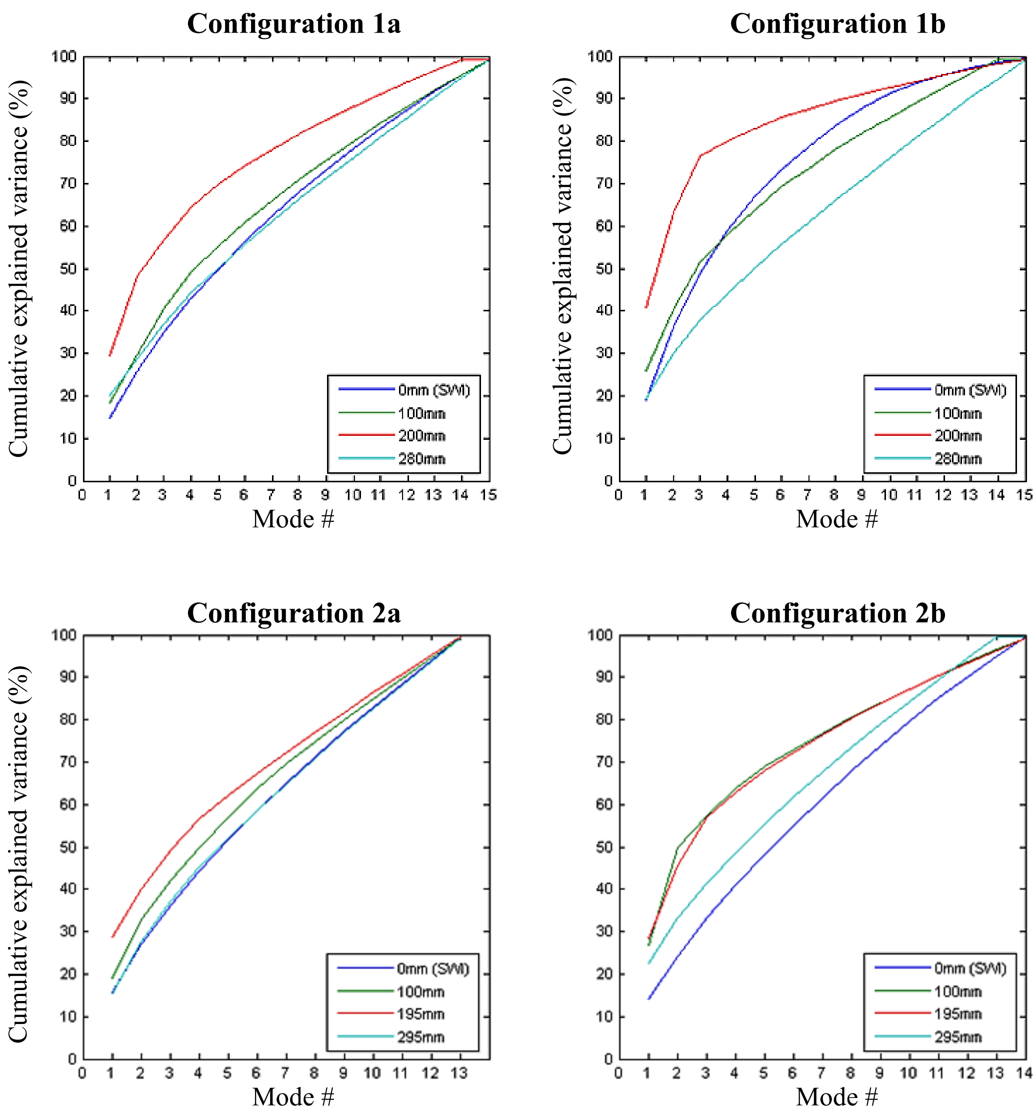


**Figure 2: Expected variance against mode for each configuration**

For the sinusoidal configurations, between 40 and 80% of the variance was explained by the first four modes for each run. Likewise, for the plane bed configurations, 40 to 60% is explained by these modes.

In general, the primary mode surface plots for both the sinusoidal and plane bedform configurations show a decay in turbulence strength with depth. At the base of the flume there is generally a slight increase in turbulence strength, as compared to the run directly above it, however it remains smaller than those measured at the surface. Low frequency turbulence less than approximately 2Hz shows very little decay with depth, whereas the rate of decay of turbulence signals appears to decrease more rapidly at higher frequencies.

For all configurations, turbulence signals of approximately 23Hz are found to be stronger below the SWI than recorded at the surface.

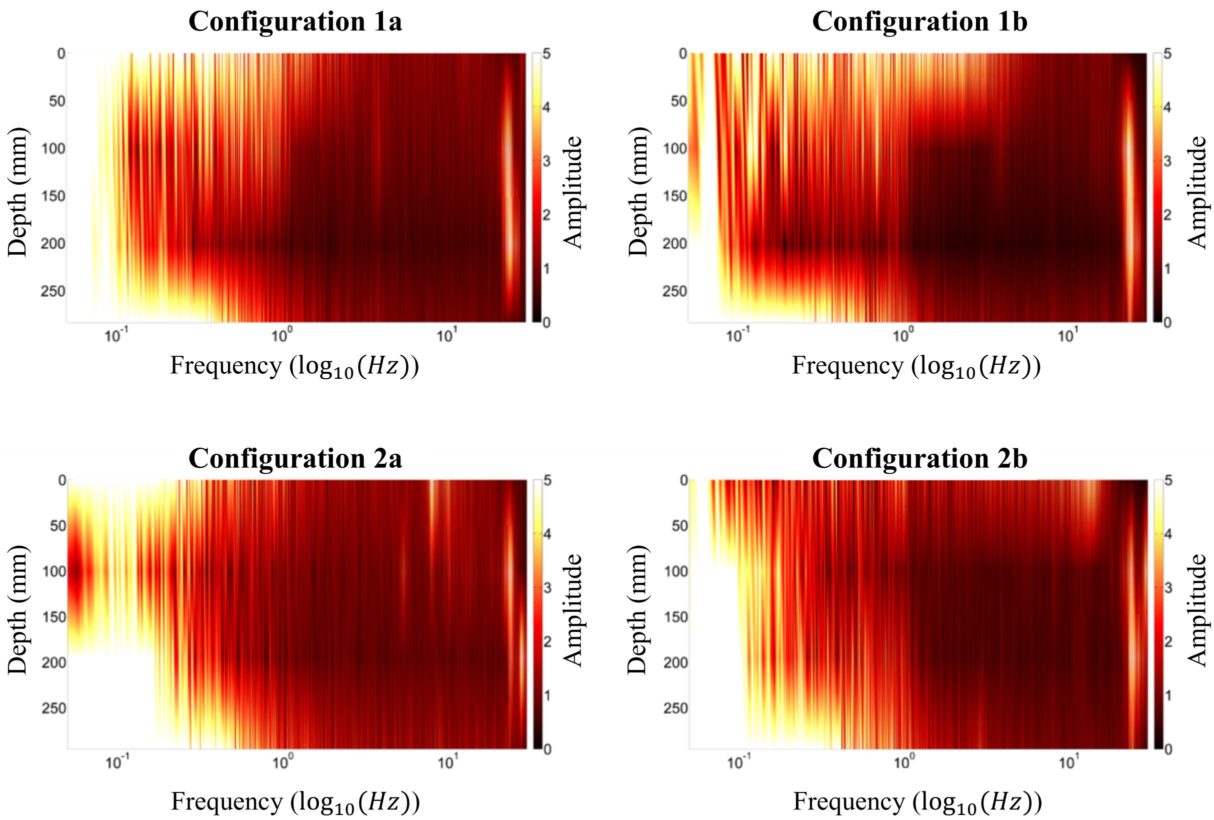


**Figure 3: Mode 1 surface plots for each configuration**

## Discussion

From the analysis it was evident that for all configurations, dynamic pressure wave propagation (representing turbulence) generally decreased with increasing frequency or depth below the SWI. The depth-dependent decay may be attributed to intensity loss—due to geometric spreading and absorption of energy by the propagation medium itself (Lurton, 2010). Combined with the refraction and diffraction of waves dependent on the velocity variations between sediment and pore water, propagation losses with depth can be generally described as exponential (Detert et al., 2010). Furthermore, the observed decay with frequency supports our hypothesis regarding low-pass filtering properties of sediment, as well as providing a physical validation of Higashino and Stefan's (2008) numerical modelling conclusions. Such observations of turbulence decay were consistent over the first four modes of variance for each configuration and not just the principal mode. We believe this observation can be partly explained by the very low compressibility of water. If water within the sediment matrix is considered compressible, it follows that any changes in pressure at a particular point will take some time to be transferred through the water column. Hence, the distance a turbulence component may penetrate the streambed must be limited by the duration of its application—expressed in its frequency. In other words, the longer a turbulence pressure component is applied, or the lower its frequency, the further it may penetrate the sediment matrix.

Many theories of hyporheic exchange, including Elliott and Brooks (1997b), Cardenas & Wilson, (2007), Bardini et al. (2012), Higashino and Stefan (2008), and Boano et al. (2007), assume water to be incompressible, thus allowing the application of the Laplace equation. Our findings suggest that such assumptions are over-simplifications of the turbulence mechanism, as pressure transmission appears to be time-dependent rather than instantaneous. Furthermore, the residence time function of the advective pumping model first proposed by Elliot and Brooks (1997b) and all subsequent iterations of their work may be refined following a more-informed understanding of the low frequency turbulence present.

While some exchange models acknowledge such limitations (e.g. Boano et al., 2011), they argue that general application of their models is correct given the region affected by turbulent pressure fluctuations is relatively shallow. This may be true in streams composed primarily of high frequency turbulence, however our findings suggest that in environments where there is a large low frequency turbulence component, the extent of the turbulence effected zone could be substantial. We found that turbulence frequencies below 2Hz undergo little decay throughout the sediment column. Any turbulence with a strong frequency component below 2Hz could thus impact stream exchange at a scale, beyond which the model accounts.

Additionally, our results also support the hypothesis that turbulence within the sediment bed is primarily generated externally in the stream, rather than within the pores of the sediment matrix. If a substantial component of turbulence was generated internally then it would be expected to manifest as an increase in turbulence strength at depths below the SWI, within the ranges of the generated frequencies. For the majority of frequencies this was not the case. Instead, it was found that the spectral distribution of turbulence signals at each depth presented a similar profile to that shown at the SWI but with reduced amplitudes. Detert et al. (2010) suggested that pore generated frequencies were in the range of 50 to 60Hz. However, as the pre-filter spectral analysis on our individual sensors showed no significant spikes at these points, it is possible this may be a function of varying sediment characteristics.

It is possible that there was some internally generated turbulence—within a small frequency band centred around 23Hz. In all experiments, analysis of the first 4 modes of variance found that turbulence strength at 23Hz was much stronger within the sediment than it was at the SWI—suggesting it may have been generated locally. For example, Figure 4 shows the spectral distribution of the primary mode of variance for Configuration 2b at each run within the 20 and 30Hz frequency range. Within this range, it can be seen that there was very little turbulence at the SWI, however spikes in turbulence strength at 23Hz are clearly visible at runs below the SWI. Given that this signal is observed across all configurations, it is unlikely that such a finding can be attributed to sensor error or interference. It is beyond the scope of this paper to determine the cause of this spike, however if it is indeed attributable to pore-generated turbulence, then it may be further elucidated with additional experiments of varying sediment type.

A feature of the surface graphs that arose at each configuration was that turbulence strength measured for runs with sensors at the base of the flume was generally higher than the run immediately above (200mm or 195mm from the SWI). We believe this can be partially attributed to the proximity of the sensors to the impermeable Perspex flume base, which may have been reflecting turbulence signals back towards the sensors.

As noted previously, the analysis was dependent on the EOF modes for each configuration being similar between runs—as judged by the similarity of explained variance outputs. In an ideal scenario, the cumulative expected variance profiles shown in Figure 2 would be closely matched by all the runs for that particular experiment; indicating that the same turbulence signals are being recorded at every run. It was found that although some runs were very similar (for example, see Configuration 2b: 100mm and 195mm), there was at minimum one run per configuration that deviated markedly from the mean. As such, a degree of caution must be taken when interpreting the results, as it cannot be guaranteed that each level is measuring the same process. However, in this case, as the outputs of the subsequent analysis align with theoretical expectations and are shown to be highly similar over the first four modes of variance, it is likely that similar signals are being measured.

In spite of each experimental configuration varying substantially in bed shape and discharge, analysis yielded very similar outputs between each. This suggests that the above mentioned relationships between turbulence strength, depth, and frequency are not just coincidental, but rather filtering processes common to all. As a result, findings may be applied to applications outside of the studied conditions.

Finally, while every effort has been made to understand the underlying physical processes, there remained some limitations within our flume experiments. In addition to the aforementioned base effects, the sediment depth was limited to 30cm, making it impossible to explore the turbulence decay over any greater depths—as would be important in physical stream scenarios. Similarly, due to the width of the flume, reflection and out-of-plane sediment heterogeneities may be causing turbulence effects not accounted for in the above detailed 2-dimensional analysis. Additionally, the study was limited to four different sensor depths per run, which reduces the accuracy of determined turbulence decay relationships. Further studies into deeper turbulence decay and various sediment types would be useful in addressing such limitations.

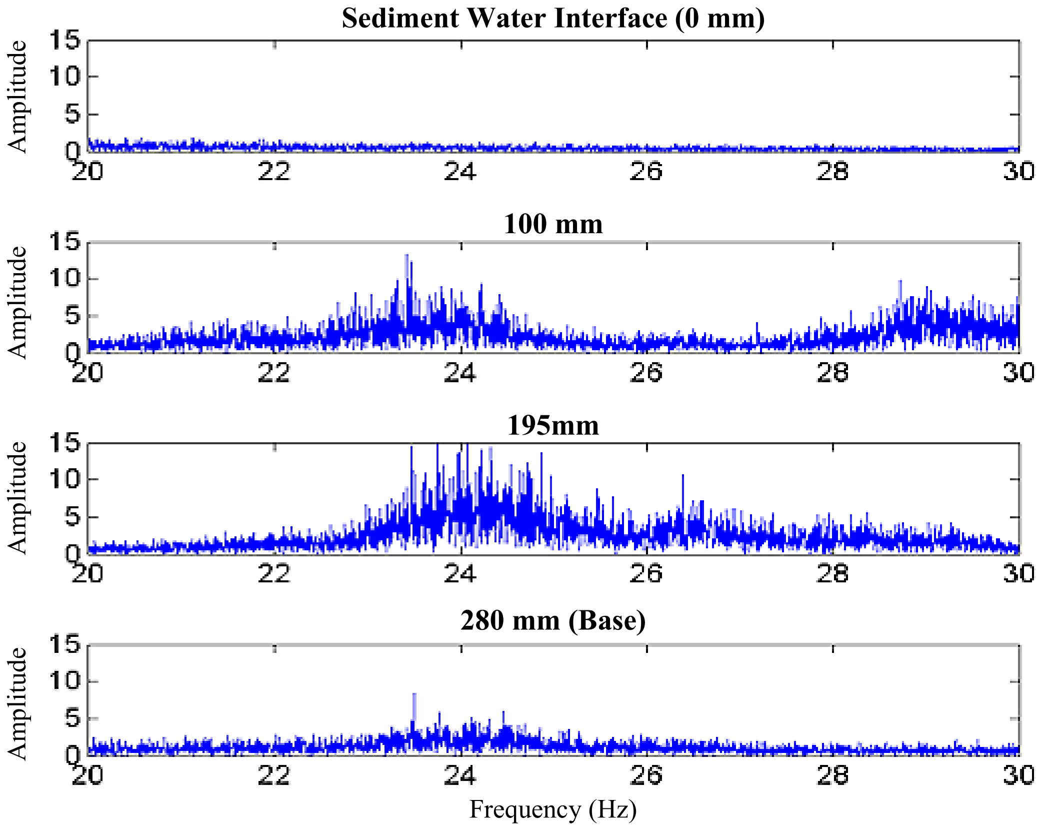


**Figure 4: Spectral distribution for primary mode of variance in Configuration 2b by run depth (20-30Hz range)**

## Conclusion

The transfer and interaction between fluid in the free stream and fluid within the porous sediment bed is ubiquitous in nature (Davidson, 2004; Cardenas & Wilson, 2007) and is essential for stream health (Bencala, 2006). While the mechanisms that govern surface flow in open channels have been studied and modelled extensively, there remains a number of knowledge gaps in the study of flows within the hyporheic region (Buss et al., 2009). A number of models have been proposed for hyporheic exchange; each based on the physical processes discussed in this paper, however many of these models (Elliott & Brooks, 1997b; Cardenas & Wilson, 2007; Bardini et al., 2012; Boano et al., 2011; Higashino & Stefan, 2008) underestimate the role of turbulent mechanisms. Through flume experiments, we show that frequencies less than 2Hz penetrate substantially into the sediment column with little decay in amplitude over our experimental depth. It is possible that this behaviour is partly attributable to the physical characteristics of the sediment and the compressibility of water. Consequently, such low frequencies may play a more important role in hyporheic exchange than previously thought. Furthermore, our data also showed increased intensity of frequencies around 23Hz within the sediment bed and not at the SWI; suggesting frequencies in this range may be a result of locally pore-generated turbulence.

We identify the need for further research into sediment-dependent relationships of turbulence decay, as our experiment was limited to a single, homogenous sediment type. Similarly, there is scope for further research into the decay profile over greater depths, as the limits to the hyporheic zone may extend further than those explored. While we identify turbulence frequencies of interest in our idealised flume experiment, additional work is required in the synthesis of these findings for model refinement.

With greater understanding of the dominant mechanisms and inputs into such hyporheic exchange models, researchers will be able to more accurately simulate such exchange processes; which has broad benefits in hyporheic exchange study and related disciplines.

# References

Bardini, L, Boano, F, Cardenas, MB, Revelli, R, & Ridolfi, L. (2012). Nutrient cycling in bedform induced hyporheic zones. *Geochimica et Cosmochimica Acta, 84*, 47-61.

Baxter, C. V., & Hauer, F. R. (2000). Geomorphology, hyporheic exchange, and selection of spawning habitat by bull trout (Salvelinus confluentus). *Canadian Journal of Fisheries and Aquatic Sciences, 57*(7), 1470-1481.

Bencala, K. E. (2006). Hyporheic exchange flows. In M. G. Anderson (Ed.), *Encyclopedia of Hydrological Sciences* (Vol. 3, pp. 1,733-1,740): John Wiley & Sons, Ltd.

Boano, F., Revelli, R., & Ridolfi, L. (2007). Bedform-induced hyporheic exchange with unsteady flows. *Advances in Water Resources, 30*(1), 148-156.

Boano, F., Revelli, R., & Ridolfi, L. (2011). Water and solute exchange through flat streambeds induced by large turbulent eddies. *Journal of Hydrology, 402*(3), 290-296.

Boulton, A. J., Datry, T., Kasahara, T., Mutz, M., & Stanford, J. A. (2010). Ecology and management of the hyporheic zone: stream–groundwater interactions of running waters and their floodplains. *Journal of the North American Benthological Society, 29*(1), 26-40.

Boulton, A. J., Findlay, S., Marmonier, P., Stanley, E. H., & Valett, H. M. (1998). The functional significance of the hyporheic zone in streams and rivers. *Annual Review of Ecology and Systematics, 29*(1), 59-81.

Brunke, M., & Gonser, T. O. M. (1997). The ecological significance of exchange processes between rivers and groundwater. *Freshwater Biology, 37*(1), 1-33.

Buss, S., Cai, Z., Cardenas, B., Fleckenstein, J., Hannah, D., Heppell, K., . . . Wood, P. (2009). The Hyporheic Handbook: a handbook on the groundwater-surface water interface and hyporheic zone for environment managers *Integrated Catchment Science Programme*. Bristol, U.K.

Cardenas, M. B., & Jiang, H. (2011). Wave-driven porewater and solute circulation through rippled elastic sediment under highly transient forcing. *Limnology & Oceanography: Fluids & Environments, 1*, 23-37.

Cardenas, M. B., & Wilson, J. L. (2007). Exchange across a sediment-water interface with ambient groundwater discharge. *Journal of Hydrology, 346*(3-4), 69-80.

Crispell, J. K., & Endreny, T. A. (2009). Hyporheic exchange flow around constructed in-channel structures and implications for restoration design. *Hydrological Processes, 23*(8), 1158-1168.

Davidson, P.A. (2004). *Turbulence : An Introduction for Scientists and Engineers: An Introduction for Scientists and Engineers*: OUP Oxford.

Detert, M, Nikora, V, & Jirka, GH. (2010). Synoptic velocity and pressure fields at the water–sediment interface of streambeds. *Journal of Fluid Mechanics, 660*, 55-86.

Elliott, A. H., & Brooks, N. H. (1997a). Transfer of nonsorbing solutes to a streambed with bed forms: Laboratory experiments. Water Resources Research, 33(1), 137-151.

Elliott, A. H., & Brooks, N. H. (1997b). Transfer of nonsorbing solutes to a streambed with bed forms: Theory. Water Resources Research, 33(1), 123-136.

Fehlman, H. M. (1985). Resistance components and velocity distributions of open channel flows over bedforms. Colorado State University.

Finkenbine, J. K., Atwater, J. W., & Mavinic, D. S. (2000). Stream health after urbanization. *Journal of the American Water Resources Association, 36*(5), 1149-1160.

Gerbersdorf, S., Hollert, H., Brinkmann, M., Wieprecht, S., Schüttrumpf, H., & Manz, W. (2011). Anthropogenic pollutants affect ecosystem services of freshwater sediments: the need for a "triad plus x" approach. *Journal of Soils and Sediments*, 1-16.

Grant, S. B., Stewardson, M. J., & Marusic, I. (2012). Effective diffusivity and mass flux across the sediment-water interface in streams. *Water Resources Research, 48*(5).

Hancock, P. J. (2002). Human impacts on the stream–groundwater exchange zone. *Environmental Management, 29*(6), 763-781.

Hendricks, S. P. (1993). Microbial ecology of the hyporheic zone: A perspective integrating hydrology and biology. *Journal of the North American Benthological Society, 12*(1), 70-78.

Higashino, M., & Stefan, H. (2008). Velocity pulse model for turbulent diffusion from flowing water into a sediment bed. *Journal of Environmental Engineering, 134*(7), 550-560.

Krause, S., Hannah, D. M., Fleckenstein, J. H., Heppell, C. M., Kaeser, D., Pickup, R., . . . Wood, P. J. (2011). Inter-disciplinary perspectives on processes in the hyporheic zone. *Ecohydrology, 4*(4), 481-499.

Lambs, L. (2004). Interactions between groundwater and surface water at river banks and the confluence of rivers. *Journal of Hydrology, 288*(3-4), 312-326.

Lesieur, M. (2008). *Turbulence in Fluids*: Springer, The Netherlands.

Lurton, X. (2010). *An introduction to underwater acoustics: Principle and applications*. Praxis Publishing, UK.

McCluskey, A. H., Stewardson, M. J., & Grant, S. B. (in prep.). A resistor model of advective pumping and turbulent penetration of bedform-induced hyporheic exchange.

Nagaoka, H., & Ohgaki, S.. (1990). Mass transfer mechanism in a porous riverbed. *Water Research, 24*(4), 417-425.

Nikora, V. (2010). Hydrodynamics of aquatic ecosystems: an interface between ecology, biomechanics and environmental fluid mechanics. *River research and applications, 26*(4), 367-384.

O'Connor, B. L., & Hondzo, M. (2008). Dissolved oxygen transfer to sediments by sweep and eject motions in aquatic environments. *Limnology and Oceanography, 53*(2), 566-578.

Packman, A. I, & Bencala, K. E. (2000). Modeling surface-subsurface hydrological interactions. *Streams and ground waters*, 45-81.

Packman, A. I., Brooks, N. H., & Morgan, J. J. (2000). A physicochemical model for colloid exchange between a stream and a sand streambed with bed forms. Water Resources Research, 36(8), 2351-2361.

Packman, A. I., & Brooks, N. H. (2001). Hyporheic exchange of solutes and colloids with moving bed forms. *Water Resources Research, 37*(10), 2591-2605.

Packman, A. I., Salehin, M., & Zaramella, M. (2004). Hyporheic exchange with gravel beds: basic hydrodynamic interactions and bedform-induced advective flows. *Journal of Hydraulic Engineering, 130*(7), 647-656.

Poole, G. C., Stanford, J. A., Running, S. W., & Frissell, C. A. (2006). Multiscale Geomorphic Drivers of Groundwater Flow Paths: Subsurface Hydrologic Dynamics and Hyporheic Habitat Diversity. *Journal of the North American Benthological Society, 25*(2), 288-303.

Pope, S. B. (2000). *Turbulent flows*: Cambridge University Press. UK.

Reidenbach, MA, Limm, M, Hondzo, M, & Stacey, MT. (2010). Effects of bed roughness on boundary layer mixing and mass flux across the sediment-water interface. *Water Resources Research, 46*(7).

Ren, J., & Packman, A. I. (2004). Stream-subsurface exchange of zinc in the presence of silica and kaolinite colloids. *Environmental Science & Technology, 38*(24), 6571-6581.

Richardson, A. J., & Humphries, P. (2010). Reproductive traits of riverine shrimps may explain the impact of altered flow conditions. *Freshwater Biology, 55*(10), 2011-2022.

Shimizu, Y., Tsujimoto, T, & Nakagawa, H. (1990). Experiment and macroscopic modelling of flow in highly permeable porous medium under free-surface flow. *J. Hydrosci. Hydraul. Eng, 8*(1), 69-78.

Stanford, J. A., & Ward, J. V. (1988). The hyporheic habitat of river ecosystems. *Nature, 335*(6185), 64-66.

Thibodeaux, L. J., & Boyle, J. D. (1987). Bedform-generated convective transport in bottom sediment.

Tonina, D., & Buffington, J. M. (2007). Hyporheic exchange in gravel bed rivers with pool-riffle morphology: Laboratory experiments and three-dimensional modeling. *Water Resources Research, 43*(1).

Triska, F. J., Duff, J. H., & Avanzino, R. J. (1993). The role of water exchange between a stream channel and its hyporheic zone in nitrogen cycling at the terrestrial-aquatic interface. *Hydrobiologia, 251*(1-3), 167-184.

Vaux, W. G. (1962). Interchange of stream and intragravel water in a salmon spawning riffle. *United States Fish and Wildlife Service Special Scientific Report - Fisheries, 405*.

Venditti, J. G., & Bennett, S. J. (2000). Spectral analysis of turbulent flow and suspended sediment transport over fixed dunes. *Journal of Geophysical Research: Oceans (1978–2012), 105*(C9), 22035-22047.

Wondzell, S. M., & Swanson, F. J. (1999). Floods, channel change, and the hyporheic zone. *Water Resources Research, 35*(2), 555-567.

Wörman, A., Packman, A.I., Johansson, H., & Jonsson, K. (2002). Effect of flow-induced exchange in hyporheic zones on longitudinal transport of solutes in streams and rivers. *Water Resources Research, 38*(1), 2-1-2-15.

Zhou, D., & Mendoza, C. (1993). Flow through porous bed of turbulent stream. *Journal of engineering mechanics, 119*(2), 365-383.

## Acknowledgements

This project has been conducted alongside ongoing research conducted by our supervisor, Alex McCluskey. We wish to thank him for his assistance with experiment design and allowing us to use much of his MatLab code. Our project would not have been possible without his tireless support, patience and valuable insight throughout this project.